NASA/CR—1998-208516

To Err is Normable: The Computation of Frequency-Domain Error Bounds From Time-Domain Data

Tom T. Hartley, Robert J. Veillette, J. Alexis De Abreu Garcia,
Amy Chicatelli, and Richard Hartmann
University of Akron, Akron, Ohio

August 1998

The NASA STI Program Office . . . in Profile

Since its founding, NASA has been dedicated to the advancement of aeronautics and space science. The NASA Scientific and Technical Information (STI) Program Office plays a key part in helping NASA maintain this important role.

The NASA STI Program Office is operated by Langley Research Center, the Lead Center for NASA's scientific and technical information. The NASA STI Program Office provides access to the NASA STI Database, the largest collection of aeronautical and space science STI in the world. The Program Office is also NASA's institutional mechanism for disseminating the results of its research and development activities. These results are published by NASA in the NASA STI Report Series, which includes the following report types:

- TECHNICAL PUBLICATION. Reports of completed research or a major significant phase of research that present the results of NASA programs and include extensive data or theoretical analysis. Includes compilations of significant scientific and technical data and information deemed to be of continuing reference value. NASA's counterpart of peer-reviewed formal professional papers but has less stringent limitations on manuscript length and extent of graphic presentations.

- TECHNICAL MEMORANDUM. Scientific and technical findings that are preliminary or of specialized interest, e.g., quick release reports, working papers, and bibliographies that contain minimal annotation. Does not contain extensive analysis.

- CONTRACTOR REPORT. Scientific and technical findings by NASA-sponsored contractors and grantees.

- CONFERENCE PUBLICATION. Collected papers from scientific and technical conferences, symposia, seminars, or other meetings sponsored or cosponsored by NASA.

- SPECIAL PUBLICATION. Scientific, technical, or historical information from NASA programs, projects, and missions, often concerned with subjects having substantial public interest.

- TECHNICAL TRANSLATION. English-language translations of foreign scientific and technical material pertinent to NASA's mission.

Specialized services that complement the STI Program Office's diverse offerings include creating custom thesauri, building customized data bases, organizing and publishing research results . . . even providing videos.

For more information about the NASA STI Program Office, see the following:

- Access the NASA STI Program Home Page at ***http://www.sti.nasa.gov***

- E-mail your question via the Internet to help@sti.nasa.gov

- Fax your question to the NASA Access Help Desk at (301) 621-0134

- Telephone the NASA Access Help Desk at (301) 621-0390

- Write to:
  NASA Access Help Desk
  NASA Center for AeroSpace Information
  7121 Standard Drive
  Hanover, MD 21076

NASA/CR—1998-208516

To Err is Normable: The Computation of Frequency-Domain Error Bounds From Time-Domain Data

Tom T. Hartley, Robert J. Veillette, J. Alexis De Abreu Garcia,
Amy Chicatelli, and Richard Hartmann
University of Akron, Akron, Ohio

Prepared under Cooperative Agreement NCC3–508

National Aeronautics and
Space Administration

Lewis Research Center

August 1998

This report is a formal draft or working paper, intended to solicit comments and ideas from a technical peer group.

This report contains preliminary findings, subject to revision as analysis proceeds.

Trade names or manufacturers' names are used in this report for identification only. This usage does not constitute an official endorsement, either expressed or implied, by the National Aeronautics and Space Administration.

Available from

NASA Center for Aerospace Information
7121 Standard Drive
Hanover, MD 21076
Price Code: A03

National Technical Information Service
5287 Port Royal Road
Springfield, VA 22100
Price Code: A03

To Err is Normable:

The Computation of Frequency-Domain Error Bounds From Time-Domain Data

Tom T. Hartley
Robert J. Veillette
J. Alexis De Abreu Garcia
Amy Chicatelli
Richard Hartmann

Department of Electrical Engineering
The University of Akron
Akron, OH 44325-3904

Abstract

This paper exploits the relationships among the time-domain and frequency-domain system norms to derive information useful for modeling and control design, given only the system step response data. A discussion of system and signal norms is included. The proposed procedures involve only simple numerical operations, such as the discrete approximation of derivatives and integrals, and the calculation of matrix singular values. The resulting frequency-domain and Hankel-operator norm approximations may be used to evaluate the accuracy of a given model, and to determine model corrections to decrease the modeling errors.

1. Introduction

Historically, system modeling has been something of an art, requiring either special knowledge of the system being considered, or a certain "intuition" into the modeling process itself. At one end of the modeling spectrum is the application of the conservation laws that describe many physical processes and environments. The resulting system models may be described by nonlinear partial differential equations in multiple spatial dimensions. These models can be simplified and converted into ordinary differential equations by finite-difference or finite-element techniques, but the resulting systems are still nonlinear and may be extremely complex. For example, in the field of Computational Fluid Dynamics (CFD), flow systems are sometimes described by literally millions of dynamic state equations. At the other end of the modeling spectrum, a control engineer may simply "guess" (or optimize) the parameters of a

low-order linear model to match the observed dynamic response of a given system. Between these two extreme approaches lie many techniques for creating a useful system model (Chicatelli and Hartley, 1997).

Regardless of which modeling approach is used, the process always yields some modeling error. Still, engineers have been able to produce successful feedback control designs for many uncertain systems, even when deprived of accurate error descriptions or estimates. Apparently, the feeling that a given system model is reasonably accurate has often been sufficient to allow a successful control design.

In recent years, though, the control systems community has been looking for stronger theoretical evidence that a feedback control designed for a nominal system model will also be suitable when applied to the actual system. Some such evidence has been found in the mathematical field of functional analysis, contributing to the evolution of the field of robust control (Doyle et al., 1992). The objective of robust control is to design a controller that will provide the desired closed-loop behavior in spite of the inevitable modeling errors and unknown disturbances that affect a system. To accomplish this, some knowledge of the system uncertainty is required. That is, the design methods that provide *a priori* guarantees of robust stability or performance invariably require prescribed bounds on the uncertainty of the system parameters or the system frequency response characteristics.

The purpose of this paper is to derive useful bounds on system modeling errors from measured data. It will be assumed throughout that the system model is intended for control design or analysis; so, the derived bounds will apply to the frequency-domain descriptions, and be useful for the application of robust control methods derived from functional analysis. However, this paper is not written for the functional analyst, but for the control engineer. Many control engineers are trained in robust control, but few are familiar with the subtle nuances of functional analysis. This paper is meant to help bridge the gap from the theoretical robust control literature to the practicing control engineer by providing the tools necessary to quickly compute error bounds that will be useful in controller design. Therefore, some mathematical results are just stated with the appropriate references, and in-depth proofs from functional analysis are avoided.

2. Signal Norms

A quantification of the errors in a control design model requires the measurement of the "size" of the error signals associated with the system. Although there are many ways to measure signal size (Doyle et al., 1992; Boyd and Barratt, 1991), the concept of signal norm is used here. The norm of a signal $y(t)$ is generally defined as

$$\|y\|_p = \left[\int_0^\infty |y(t)|^p dt\right]^{1/p}. \tag{1}$$

This is the general definition of the p-norm, where p is usually a positive integer. Note that $y(t)$ is assumed to be defined for all $t \geq 0$. For most purposes, $y(t)$ is assumed zero for $t < 0$.

Of all the p-norms, the 1-norm, the 2-norm, and the infinity-norm are the most useful, mainly because of their simple intuitive interpretations. These will be discussed below.

The 1-norm

Setting p=1 in the general definition (1) yields the definition of the 1-norm of $y(t)$ as

$$\|y\|_1 = \int_0^\infty |y(t)| dt. \tag{2}$$

Thus the 1-norm of a signal is equal to the integral of the absolute value of the signal. If, for example, $y(t)$ represents the force applied over time to a body in motion, then $\|y\|_1$ may represent the total effort or fuel expended.

For the 1-norm of a signal to be finite, the signal must eventually decay to zero.[1] For signals that do not decay to zero, such as step functions or sinusoids, the integral diverges and the 1-norm is considered infinite.

The 2-norm

Setting p=2 in the general definition (1) yields the definition of the 2-norm of $y(t)$ as

$$\|y\|_2 = \left[\int_0^\infty |y(t)|^2 dt\right]^{1/2}. \tag{3}$$

[1] This statement assumes the signal is absolutely continuous, which holds for all signals produced as the outputs of ordinary or partial differential equations. The condition of absolute continuity is assumed throughout this paper.

The 2-norm is closely related to the energy of a signal. If, for example, $y(t)$ is a voltage applied to a resistive load, then $\|y\|_2^2$ is proportional to the energy delivered to the load. The 2-norm is also related to the variance, which is defined as

$$\mathrm{var}(y) = \lim_{T\to\infty}\left[\frac{1}{T}\int_0^T |y(t)|^2 dt\right], \tag{4}$$

and to the RMS value (or standard deviation), which is the square-root of the variance. Note that, because of the division by the time interval T in (4), the variance and the RMS value may be finite for signals such as steps or sinusoids that do not decay. However, like the 1-norm, the 2-norm is finite only for signals that decay to zero. The variance and the RMS value are mentioned here to provide a clearer understanding of the 2-norm, but will not be used in that which follows.

The 2-norm of a signal may be defined equally well in the frequency domain as

$$\|Y(j\omega)\|_2 = \left(\frac{1}{2\pi}\int_{-\infty}^{\infty} |Y(j\omega)|^2 d\omega\right)^{\frac{1}{2}}, \tag{5}$$

where $Y(j\omega)$ is the Fourier transform of $y(t)$, and the integration is now carried out over all frequencies. The factor of 2π is for the purpose of normalization. A simple mathematical link between the time-domain and frequency-domain signal representations is established by Parseval's theorem, which states that the signal energy in the time domain is equal to the signal energy in the frequency domain. This may be written in terms of the 2-norms simply as

$$\|y\|_2 = \|Y(j\omega)\|_2 . \tag{6}$$

The infinity-norm

Letting p approach infinity in the general p-norm definition (1) yields the infinity-norm of $y(t)$ as

$$\|y\|_\infty = \lim_{p\to\infty}\left[\int_0^\infty |y(t)|^p dt\right]^{1/p} . \tag{7}$$

Although this may at first appear dubious, it is resolvable. For large p, the maximum values of $y(t)$ are emphasized in the integral far more than the smaller values; so, the integral is

approximately proportional to the maximum value of $y(t)$ raised to the power p. Taking the p^{th} root and letting p approach infinity yields

$$\|y\|_\infty = \max_t |y(t)|. \tag{8}$$

Thus, the infinity-norm of a signal is simply the largest value of the signal in magnitude.[2] In other words, the infinity-norm of a signal represents a bound on the signal amplitude for all time. Unlike the 1-norm and the 2-norm, the infinity-norm of a signal may be finite even though the signal does not decay.

Example

As an example, consider the function

$$y(t) = \exp(-t) - \exp(-2t),\ t \geq 0,$$

whose graph is shown in Figure 1(a). The 1-norm of this function is calculated as

$$\|y\|_1 = \int_0^\infty |\exp(-t) - \exp(-2t)| dt = \frac{1}{2},$$

which is equal to the area under the graph of $y(t)$. The 2-norm is calculated as

$$\|y\|_2 = \left(\int_0^\infty |\exp(-t) - \exp(-2t)|^2 dt \right)^{\frac{1}{2}} = \sqrt{\frac{1}{12}}.$$

The square of the 2-norm is the area under $|y(t)|^2$ in the time domain, shown in Figure 1(b). This is equal to the area under $|Y(j\omega)|^2 / 2\pi$ in the frequency domain, shown in Figure 1(c). The infinity norm is the maximum value,

$$\|y\|_\infty = \frac{1}{4},$$

which occurs at time $t = \ln(2)$.

3. Two System Norms

It is now necessary to define the norms of a system, as measures of the size of the system. For a system represented by a transfer function, the system norms can be defined in the

[2] To be more precise, the infinity norm should be defined using the *supremum* (sup), or least upper bound, rather than the maximum value (max) of the signal. This would take care of the case where the signal does not achieve any maximum value, but only approaches a certain least upper bound.

frequency domain similar to the signal norms in the time domain. It turns out that such a system norm may be interpreted as a gain of the system. Control engineers understand the gain of a system as a function of the input frequency, but this assumes the system inputs to be sinusoidal. A more general definition of the system gain is provided by the system norms (Doyle et al., 1992; Boyd and Barratt, 1991).

Assume that a given system is linear, time-invariant, and causal, and is described by the transfer function $H(s)$. Assume also that the system is stable, so that all the poles of $H(s)$ lie in the left half of the complex plane. The frequency response of the system, denoted by $H(j\omega)$, is the transfer function $H(s)$ evaluated on the imaginary axis, $s=j\omega$. The system impulse response, denoted by $h(t)$, is the inverse Laplace transform of $H(s)$, or the inverse Fourier transform of $H(j\omega)$.

The Frequency-domain Infinity-norm

Now the infinity-norm already defined for time-domain signals may be applied in the frequency domain and used as a system norm. Replacing time with frequency in the definition of the infinity-norm (8) yields the new definition

$$\|H(j\omega)\|_\infty = \max_\omega |H(j\omega)|, \tag{9}$$

where $|H(j\omega)|$ is the magnitude of the frequency response at the frequency ω. Thus the infinity-norm in the frequency domain is equal to the largest magnitude of the frequency response over all frequencies. Graphically, it represents the highest peak in the (Bode) magnitude plot of the transfer function, or the magnitude of the point on the Nyquist plot farthest from the origin in the complex plane. The 1-norm and the 2-norm of the frequency response are also commonly defined by analogy with the time-domain definitions, but these will not be considered here.

It is clear that the frequency-domain infinity-norm of a system is the maximum possible system gain when considering only sinusoidal excitations. It also happens to be a useful measure of the system gain for inputs that are not sinusoidal. Let a general system input be denoted by $u(t)$ and the system output by $y(t)$, both of which are assumed to be scalars. (The vector case will be considered later.) The Fourier transforms of $u(t)$ and $y(t)$ are denoted as $U(j\omega)$ and $Y(j\omega)$, respectively. With these definitions, it is well known that

$$Y(j\omega) = H(j\omega)U(j\omega), \tag{10}$$

which yields

$$|Y(j\omega)| = |H(j\omega)||U(j\omega)|. \tag{11}$$

Observing that the frequency response magnitude $|H(j\omega)|$ at any frequency is no greater than the infinity-norm of the system, we obtain

$$|Y(j\omega)| \le \|H(j\omega)\|_\infty |U(j\omega)|. \tag{12}$$

Note that the frequency-domain p-norms of $Y(j\omega)$ and $U(j\omega)$ can be defined just as for the transfer function $H(j\omega)$. Squaring both sides of the above inequality, integrating over frequency, and taking the square root yields the relation

$$\|Y(j\omega)\|_2 \le \|H(j\omega)\|_\infty \|U(j\omega)\|_2. \tag{13}$$

This inequality is a bound on the output energy in the frequency domain. By Parseval's Theorem, this bound also holds in the time-domain as

$$\|y\|_2 \le \|H(j\omega)\|_\infty \|u\|_2. \tag{14}$$

Thus the infinity-norm of the system frequency response provides a bound on the ratio of output energy to input energy in the time domain, which is a useful measure of the system gain.

The Time-domain 1-norm

A second measure of the system gain can be obtained directly from the time-domain description of the system. The time-domain equivalent of (10) is the convolution integral

$$y(t) = \int_0^t h(\tau)u(t-\tau)d\tau, \tag{15}$$

where $h(t)$ is the impulse response of the system. Taking the magnitude of both sides, we obtain

$$|y(t)| = \left| \int_0^t h(\tau)u(t-\tau)d\tau \right|. \tag{16}$$

Then the triangle inequality yields

$$|y(t)| \le \int_0^t |h(\tau)u(t-\tau)|d\tau. \tag{17}$$

Since the input function $u(t)$ is bounded by its infinity-norm (maximum value), the inequality (17) yields

$$|y(t)| \le \int_0^t |h(\tau)| \|u\|_\infty \, d\tau \,. \tag{18}$$

The norm of $u(t)$ can be factored out to give

$$|y(t)| \le \left(\int_0^t |h(\tau)| d\tau \right) \|u\|_\infty \,. \tag{19}$$

The integral in (19) is at its largest as t goes to infinity, at which point it approaches the 1-norm of the system impulse response. Consequently, the above inequality yields

$$|y(t)| \le \|h\|_1 \, \|u\|_\infty \,. \tag{20}$$

Since this bound holds for all time t, it also holds for the maximum value of $y(t)$, its time-domain infinity-norm. Hence, (20) yields

$$\|y\|_\infty \le \|h\|_1 \, \|u\|_\infty \,. \tag{21}$$

Thus the 1-norm of the system impulse response is another useful measure of the system gain, as it bounds the maximum output value for a given maximum input value in the time domain.

Relationship between the System Norms

The infinity-norm of the system frequency response bounds the input-output energy ratio, and the 1-norm of the system impulse response bounds the input-output amplitude ratio in the time domain. It is now shown that, for a given system, the frequency-domain infinity-norm is always less than the time-domain 1-norm.

The Fourier transform of the system impulse response is given by

$$H(j\omega) = \int_0^\infty h(t) \exp(-j\omega t) dt \,. \tag{22}$$

Taking the magnitude of both sides and using the triangle inequality yields

$$|H(j\omega)| = \left| \int_0^\infty h(t) \exp(-j\omega t) dt \right| \le \int_0^\infty |h(t) \exp(-j\omega t)| dt = \int_0^\infty |h(t)| |\exp(-j\omega t)| dt \,. \tag{23}$$

The exponential inside the integral has a magnitude of unity for all frequencies; therefore, this yields

$$|H(j\omega)| \leq \int_0^\infty |h(t)|dt \equiv \|h\|_1 . \tag{24}$$

As this inequality holds for all frequencies, the left side may be replaced by the frequency-domain infinity-norm. This yields the final relation

$$\|H(j\omega)\|_\infty \leq \|h\|_1 . \tag{25}$$

Thus the frequency-domain system norm is bounded by the time-domain system norm. This relationship will be useful for obtaining an estimate of the system infinity-norm from time-domain experimental data or simulation results.

4. Errors in Modeling

The goal of this paper is to determine bounds on the error incurred in the modeling process. The modeling error can be defined simply as the difference between the approximate linear model and the real system or a realistic "truth model"; see Figure 2. The linear model has been extracted from the truth model, or from actual measured data. In general, the real system or truth model is nonlinear and of high order, whereas the linear model is relatively simple. For a given input signal, with the two systems running in parallel, an output error signal can be determined.

Sources of Error

The greatest part of the inaccuracy of the low-order linear model probably results from the linear approximation. Because the true system is not linear, the error depends upon the size of the system input. It is difficult to tell at the modeling stage how large the input can be without introducing unacceptably large errors. Another source of inaccuracy arises from the reduction of the system order, or elimination of system state variables. The determination of a low-order model suitable for control system design usually requires a significant reduction of order from the real system model, which can have millions of state variables in the case of a CFD model. Fortunately, the model-order reduction usually contributes relatively little to the modeling error. In any event, if standard model-order reduction techniques are used, the resulting errors are within known bounds (Glover and Partington, 1987; Glover et al., 1988).

Frequency-domain Representation of Error

The system gains introduced in Section 3 are now discussed in connection with the modeling error and its bounds. The system model $H(s)$ has a known frequency response $H(j\omega)$ that can be represented by magnitude and phase (Bode) plots or, better yet, by a polar (Nyquist) plot in the complex plane. At each point on the Nyquist plot, there will be some error owing to the inaccuracy in $H(j\omega)$ at the corresponding frequency ω. This error, denoted $E(j\omega)$, is the frequency response of the error system of Figure 2. The largest magnitude of the error over all frequencies is the frequency-domain infinity-norm of the error, represented by $\|E(j\omega)\|_\infty$. Even if this norm is known, it is only a bound on the magnitude of the error, and contains no information about the phase of the error. Consequently, all possible phase angles must be considered, from 0 to 2π. Graphically, in the Nyquist plane, the error bound at each frequency is represented by a circle of radius $\|E(j\omega)\|_\infty$, centered on the Nyquist plot at that frequency. This means that the true frequency response of the system would lie within a "tube" in the Nyquist plane, as shown in Figure 3.

This frequency-domain view of the error system presupposes that the true system is linear, which it is not. Nevertheless, this is the view that we shall adopt. The linear system norms can be thought of as providing a first-order approximation of the size or gain of a nonlinear system; they are useful in practice for evaluating and improving linear models of nonlinear systems, as the example at the end of the paper illustrates.

Approximating the Modeling Error

The problem now is to obtain $\|E(j\omega)\|_\infty$. To obtain it directly would require knowing the error, in Figure 2, for all input sinusoidal frequencies. But it is not practical to apply sinusoidal inputs over a wide frequency range to either a real system or its detailed truth model. An alternative approach would be to make use of the results of the last section to obtain the bound

$$\|E(j\omega)\|_\infty \le \|e\|_1, \tag{26}$$

where $e(t)$ is the response of the error system to an impulse input. If the time-domain 1-norm of the error system can be obtained, then it can be used as a frequency-domain error bound.

Unfortunately, it may be difficult to obtain the impulse response of the error. This is particularly true if it would require an experiment with the actual physical hardware, as

generating and applying an impulse input may be problematical. On the other hand, accurate step responses are usually either known or readily obtainable from the physical hardware or truth-model simulations.

Assuming again that the system is reasonably linear, the impulse response is simply the time-derivative of the step response multiplied by the chosen time units. This may be seen from Figures 4 and 5, where the operator s represents the differentiation together with the multiplication by the time units. The multiplication by the time units is necessary to preserve the overall units of the system inputs and outputs, which must be equivalent in either figure. The same time units must be assumed in both figures; that is, those units in which the impulse input is assumed to have unit area must be the same ones used to correct the system output units after differentiating the step response. It is safest to choose a single unit of time as the standard for the entire analysis, and stick to it throughout.

A discrete-time approximation of the impulse response $e(t)$ may be obtained from the step response $e_{step}(t)$ via the numerical differentiation

$$e(kT) = \frac{e_{step}(kT) - e_{step}((k-1)T)}{T}. \tag{27}$$

Here, the units of $e(kT)$ are taken to be the same as those of $e_{step}(kT)$, assuming that T is evaluated in the standard time units. The integral for the 1-norm of the error is then approximated by a sum as

$$\|e(t)\|_1 = \int_0^\infty |e(t)|dt \cong \sum_{k=0}^{\infty} T|e(kT)|. \tag{28}$$

This approximation of the time-domain 1-norm of the system error provides a bound for the frequency-domain infinity-norm error, which can then be used on the Nyquist plot. The interpretation of the frequency-domain error bounds in the modeling process is now discussed.

Referring back to Figure 3, the Nyquist plot contains the frequency response of the low-order linear system model, as well as the system error bound as a "tube" in the Nyquist plane. The radius of this "tube" represents the worst-case error magnitude over all frequencies. The particular frequency or frequencies for which this worst-case error occurs is not known; theoretically, the largest error could occur at every frequency. The low-order system model can be said to be relatively accurate at frequencies where its magnitude is larger than the error bound.

Thus, to determine a range of frequencies over which the low-order linear system model is relatively accurate, the error bound circles can be removed from the Nyquist plot and a single error bound circle drawn at the origin of the Nyquist plane, as in Figure 6. The low-order linear system model is then considered relatively accurate as long as its Nyquist plot stays outside the error bound circle at the Nyquist plane origin. At those frequencies for which the Nyquist plot lies inside this error bound circle, the model is considered relatively inaccurate.

Another interesting interpretation of the error bound in the time domain comes from the time-domain system gain relation

$$\|\varepsilon(t)\|_\infty \le \|e(t)\|_1 \|u(t)\|_\infty , \tag{29}$$

where $\varepsilon(t)$ is the output error in response to an arbitrary input $u(t)$. According to the bound, for inputs $u(t)$ that do not exceed unit amplitude, the time-domain 1-norm of the error impulse response is an upper bound on $|\varepsilon(t)|$ for all time. This bound assumes the error system to be approximately linear, and so may be most applicable for small inputs. In fact, the bound is usually quite conservative; so, it may still be usable for larger inputs, despite the nonlinearity of the real system model.

Error Incurred in Further Reduction

It is sometimes desirable to further simplify a model by a model-order reduction after the initial linear approximation. In this situation, the frequency-domain error bounds simply add, as

$$\|E_{total}(j\omega)\|_\infty \le \|E_{linearization}(j\omega)\|_\infty + \|E_{reduction1}(j\omega)\|_\infty + \|E_{reduction2}(j\omega)\|_\infty + \cdots . \tag{30}$$

This means that an approximation of an approximation increases the error bound by the magnitude of the additional error bound. This approach stands as an alternative to recalculating the error bound by applying Equations (27-28) to the step response error of the newly reduced-order system.

Modeling Errors in Control Design

The field of robust control is concerned largely with accounting for unknown modeling errors in the control design process (Doyle et al., 1992). A simple discussion of the effect of modeling errors on the feedback control system design is now presented. The closed-loop system is assumed to be of the form given in the block diagram of Figure 7. In the diagram, $H(s)$ is the low-order linear system model, $E(s)$ is the modeling error, and the sum $H(s)+E(s)$

represents the real system. Neither the modeling error $E(s)$ nor its infinity-norm $\|E(j\omega)\|_\infty$ is precisely known, but the time-domain 1-norm $\|e\|_1$ can be found, and is a bound on the infinity-norm. Therefore, the worst-case error at any frequency may be represented as

$$E_{worst}(j\omega) \approx \|e\|_1 \exp(j\theta), \tag{31}$$

where the phase θ of the error is unknown. The expression (31) represents the error circles of radius $\|e\|_1$ in the Nyquist plane.

To determine the stability of the closed-loop system, the frequency response of the loop transfer function is plotted in the Nyquist plane. The loop transfer function frequency response is given by

$$T(j\omega) = G(j\omega)[H(j\omega) + E(j\omega)], \tag{32}$$

where $G(s)$ is the compensator transfer function. To represent the largest possible deviation of $T(j\omega)$ from its nominal value, we replace $E(j\omega)$ by the worst-case error, to obtain

$$T(j\omega) = G(j\omega)\left[H(j\omega) + \|e\|_1 \exp(j\theta)\right]. \tag{33}$$

This expression yields the worst-case loop transfer function as

$$T(j\omega) = G(j\omega)H(j\omega) + |G(j\omega)|\|e\|_1 \exp(j\theta). \tag{34}$$

The last term in (34) represents the uncertainty in the loop transfer function. Note that $G(j\omega)$ has been replaced by $|G(j\omega)|$, since the arbitrary angle θ already accounts for the compensator phase. The uncertainty is represented in the Nyquist plane by error-bound circles whose radii at each frequency are given by $|G(j\omega)|\|e\|_1$. Thus, around the Nyquist plot there is a tube whose radius changes with frequency, as shown in Figure 8. To guarantee stability, the compensator must be designed so that this tube avoids the critical point $-1+j0$ in the Nyquist plane.

In some cases, the analysis may be simplified somewhat by considering the frequency-domain infinity-norm of the controller. Replacing $|G(j\omega)|$ by its largest value $\|G(j\omega)\|_\infty$ yields the worst-case loop transfer function

$$T(j\omega) = G(j\omega)H(j\omega) + \|G(j\omega)\|_\infty \|e\|_1 \exp(j\theta). \tag{35}$$

Using this expression, the Nyquist plot of the nominal compensated plant can be plotted with error bound circles of equal radii, as shown in Figure 9. The radius of each circle is the product of the compensator and error norms. If the resulting tube in the Nyquist plane misses the critical

point $-1+j0$, then the system is guaranteed to be stable for the given uncertainty of the plant. An equivalent condition is shown in Figure 10, where the error bound circles have been removed from the frequency response, and a single circle has been drawn centered at the critical point in the Nyquist plane. Thus, the major effect of the uncertainty error bound is to effectively enlarge the critical point in the Nyquist plane to a circle. This circle must be avoided by the closed-loop frequency response to guarantee stability in the presence of the bounded modeling errors.

In many control systems, such as those that require integral control for tracking, the compensator has a very large infinity-norm because of a pole on or near the $j\omega$ axis. In this case, the tube in the Nyquist plane would consist of a very large circle at each point of the Nyquist plot, or equivalently at the critical point in the Nyquist plane. Then the simplified condition derived from (35), while still valid, is not particularly useful, and the circles of unequal radii derived from (34) should be used.

5. Norms Based on the Hankel Operator

This section presents a few more system norms based on the definition of the Hankel operator of the system (Partington, 1988). If the impulse response of a system is denoted by $h(t)$, the Hankel operator Γ of the system is defined by the relation

$$(\Gamma u)(t) = \int_0^\infty h(t+\tau)\, u(-\tau) d\tau\,, \quad t \geq 0. \tag{36}$$

This is an integral operator mapping all past inputs u into future outputs Γu. That is, the output Γu of the Hankel operator is the same as the output of the system for $t > 0$ in response to an input u applied only for $t < 0$.

The Hankel Singular Values

The Hankel operator turns out to be rather easy to work with, and also useful in finding reduced-order models for complex systems. To this end, we will write the expressions that define the eigenvalues and eigenvectors of the Hankel operator. The n^{th} eigenvector of the Hankel operator is an input function $u_n(t)$ defined for $t \leq 0$ such that

$$\sigma_n u_n(-t) = \int_0^\infty h(t+\tau)\, u_n(-\tau)\, d\tau\,, \quad t \geq 0, \tag{37}$$

where the scalar σ_n is the corresponding eigenvalue. The eigenvector relation can equally well be written as

$$\sigma_n v_n(\tau) = \int_0^\infty h(t+\tau)\, v_n(t)\, d\tau\,, \quad \tau \geq 0, \tag{38}$$

where $v_n(t)$ is defined for $t \geq 0$. The functions $u_n(t)$ and $v_n(t)$ are essentially the same, except that one is defined for positive t and the other for negative t.

Because the kernel $h(t+\tau)$ of the Hankel operator depends on both t and τ in the same way, the operator is called "self-adjoint," which means that it has many of the properties of a symmetric matrix. Therefore, it turns out that the eigenvectors of the Hankel operator are equivalent to its singular vectors, and are mutually orthogonal. The eigenvector relations for the Hankel operator may therefore be written in the form of singular vector relations as

$$\sigma_n v_n(t) = \int_0^\infty h(t+\tau)\, u_n(-\tau)\, d\tau\,, \quad t \geq 0, \tag{39}$$

$$\sigma_n u_n(-\tau) = \int_0^\infty h(t+\tau)\, v_n(t)\, dt\,, \quad \tau \geq 0, \tag{40}$$

where the functions u_n and v_n are known, respectively, as the n^{th} left and right Hankel singular vectors, and $u_n(-t) = v_n(t)$ for $t \geq 0$. The Hankel singular vectors are also referred to as the Schmidt pairs of the Hankel operator. The scalar σ_n is known as the n^{th} Hankel singular value of the system. The number of nonzero Hankel singular values (and corresponding Schmidt pairs) is equal to the order of the system. The operator describing a spatially distributed system may have infinitely many nonzero Hankel singular values.

The Hankel singular values of a real system are always real and positive, and are usually listed in decreasing order so that σ_1 is the largest. They are related to the gain of the system, and are used to define several system norms, as follows.

The Hankel norm of a system with the transfer function $H(s)$, denoted $\|H(s)\|_H$, is defined to be the largest Hankel singular value; that is,

$$\|H(s)\|_H = \sigma_1\,. \tag{41}$$

This norm represents the maximum ratio of future output energy to past input energy [Boyd and Barratt]. In mathematical terms, one would say that the Hankel norm of the system is the induced 2-norm of the Hankel operator, or

$$\|H(s)\|_H = \|\Gamma\| = \max_u \frac{\|y\|_2}{\|u\|_2} = \sigma_1 . \tag{42}$$

Another norm of $H(s)$ related to the Hankel operator is the nuclear Hankel norm, denoted $\|H(s)\|_{N-H}$. It is defined as the sum of the Hankel singular values. That is,

$$\|H(s)\|_{N-H} = \sum_{n=1}^{\infty} \sigma_n . \tag{43}$$

The Hankel operator is said to be nuclear if its nuclear norm is finite.

Yet another norm of $H(s)$ related to the Hankel operator is the Hilbert-Schmidt Hankel norm, denoted $\|H(s)\|_{H-S-H}$. It is defined as the square root of the sum of the squares of the Hankel singular values. That is,

$$\|H(s)\|_{H-S-H} = \left(\sum_{n=1}^{\infty} \sigma_n^2 \right)^{1/2} . \tag{44}$$

This can be thought of as the Frobenius norm of the Hankel operator, and is also referred to as the Frobenius-Hankel norm, denoted $\|H(s)\|_{F-H}$. If this norm is finite, the Hankel operator is said to be Hilbert-Schmidt. Interestingly enough, the square of the Hilbert-Schmidt Hankel norm is equal to the time-weighted impulse response energy,

$$\|H(s)\|_{H-S-H}^2 = \sum_{n=1}^{\infty} \sigma_n^2 = \int_0^{\infty} t\,[h(t)]^2\, dt . \tag{45}$$

It can be shown that this quantity is also equal to the area inside the Nyquist plot of the frequency response of the system (Hanzon, 1992).

The above system norms are known (Glover et al., 1988) to be related by the inequalities

$$\|H(s)\|_H \le \|H(j\omega)\|_\infty \le \|h(t)\|_1 \le 2\,\|H(s)\|_{N-H} . \tag{46}$$

The Hankel Approximation of a System

If the Schmidt pairs of an integral operator are known, the kernel of the operator is given by an expansion similar to the singular-value decomposition of a matrix. In the case of the Hankel operator, the kernel is the system impulse response, and is expanded as

$$h(t+\tau)=\sum_{n=1}^{\infty}\sigma_n v_n(t)u_n(-\tau). \tag{47}$$

This is called the Hilbert-Schmidt expansion of the Hankel operator. Given this expansion, an approximation of the impulse response may be found by truncating the series as

$$\tilde{h}(t+\tau)=\sum_{n=1}^{q}\sigma_n v_n(t)u_n(-\tau), \tag{48}$$

where q is the order of the approximation. A system with the impulse response $h(t)$ will constitute a q^{th}-order model of the original system with impulse response $\tilde{h}(t)$. Based on this idea, Glover et al. (1988) derived a state-variable description of this q^{th}-order Hankel approximation, solely from the first q Hankel singular values and the Schmidt pairs of the original system. The resulting state-variable parameters are

$$B_i=\sigma_i v_i(0) \tag{49}$$

$$C_i=u_i(0) \tag{50}$$

$$A_{ii}=-\frac{1}{2}u_i^2(0) \tag{51}$$

$$A_{ij}=\frac{B_i^*B_j-\sigma_i^2C_i^*C_j}{\sigma_i^2-\sigma_j^2}, \tag{52}$$

where the indices i and j are bounded by q, the order of the approximation. The given state-variable parameters describe a balanced realization in output normal form. Notice that the Schmidt pairs are evaluated at time $t=0$. It is assumed that the Schmidt pairs are normalized, so that $\|u_i\|_2=\|v_i\|_2=1$ for each i.

The accuracy of the Hankel approximation is measured by the truncated Hankel singular values. Specifically, if $H(s)$ describes the original system and $\tilde{H}(s)$ the q^{th}-order Hankel approximation, the Hankel norm of the approximation error is given by

$$\left\|H(s)-\tilde{H}(s)\right\|_H=\sigma_{q+1}, \tag{53}$$

where σ_{q+1} is the largest Hankel singular value of the original system that has not been taken into account in the approximation. Further, a frequency-domain bound is given by

$$\left\|H(s)-\tilde{H}(s)\right\|_{\infty} \leq 2\sum_{n=q+1}^{\infty}\sigma_n \,. \tag{54}$$

Application to the Error System

If $h(t)$ represents the impulse response of the error system $E(s)$, and the associated Schmidt pairs and Hankel singular values can be found, then the upper and lower bounds on the frequency-domain error norm are given as

$$\left\|E(s)\right\|_{H} \leq \left\|E(j\omega)\right\|_{\infty} \leq 2\left\|E(s)\right\|_{N-H} \,. \tag{55}$$

Furthermore, the formulas (49-52) may be used to determine a system $\tilde{E}(s)$ of order q that approximates the error system. Recall that the actual error system is not precisely known, and may be of extremely high order. The q^{th}-order approximate system $\tilde{E}(s)$ is used as a correction; that is, it may be added in parallel to the system model to decrease the error. The error remaining after the Hankel correction is given as $\bar{E}(s) = E(s) - \tilde{E}(s)$, and is bounded in the frequency domain by

$$\left\|\bar{E}(j\omega)\right\|_{\infty} \leq 2\sum_{n=q+1}^{\infty}\sigma_i \,, \tag{56}$$

as well as by

$$\left\|\bar{E}(j\omega)\right\|_{\infty} \leq \left\|e(t)-\tilde{e}(t)\right\| \,, \tag{57}$$

where $\tilde{e}(t)$ is the impulse response of the correction $\tilde{E}(s)$.

Approximation of the Hankel Operator

So far, we have assumed that the Hankel singular values and singular vectors are known. However, finding them usually requires a linear system description in state-variable form. Lacking this, we turn to numerical methods for approximating the calculations of Glover et al. (1988).

The Fredholm approach to solving integral equations (Lovitt, 1950) is adapted for obtaining a useful approximation. Basically, the Fredholm approach is to divide the integration limits for the Hankel operator into evenly spaced intervals in t and τ, and then to add up the

resulting samples of the kernel using the rectangular rule for integration. The integral relationship for the eigenvalues and eigenvectors,

$$\sigma_n u_n(t) = \int_0^\infty h(t+\tau)\, u_n(\tau)\, d\tau, \tag{58}$$

is sampled in t and τ with a sampling period T, to obtain

$$\begin{aligned}
\hat{\sigma}_n \hat{u}_n(0) &= T\left[h(0+0)\hat{u}_n(0) + h(0+1)\hat{u}_n(1) + \cdots + h(0+N)\hat{u}_n(N)\right] \\
\hat{\sigma}_n \hat{u}_n(1) &= T\left[h(1+0)\hat{u}_n(0) + h(1+1)\hat{u}_n(1) + \cdots + h(1+N)\hat{u}_n(N)\right] \\
&\vdots \\
\hat{\sigma}_n \hat{u}_n(N) &= T\left[h(N+0)\hat{u}_n(0) + h(N+1)\hat{u}_n(1) + \cdots + h(N+N)\hat{u}_n(N)\right].
\end{aligned} \tag{59}$$

In this sampled approximation, the eigenvalues σ_n and eigenvectors $u_n(t)$ are replaced by their approximate representations $\hat{\sigma}_n$ and $\hat{u}_n(k)$. Rewriting these equations in matrix form yields the eigenvalue relation

$$\hat{\sigma}_n [u_n] = TH\,[u_n], \tag{60}$$

where

$$[u_n] = \begin{bmatrix} \hat{u}_n(0) \\ \hat{u}_n(1) \\ \vdots \\ \hat{u}_n(N) \end{bmatrix} \tag{61}$$

is the n^{th} eigenvector and $\hat{\sigma}_n$ the corresponding eigenvalue of the matrix TH, with

$$H = \begin{bmatrix} h(0) & h(1) & \cdots & h(N) \\ h(1) & h(2) & \cdots & h(N+1) \\ \vdots & \vdots & \ddots & \vdots \\ h(N) & h(N+1) & \cdots & h(N+N) \end{bmatrix}. \tag{62}$$

This eigenvalue problem may also be written as

$$(\hat{\sigma}_n I - TH)[u_n] = 0. \tag{63}$$

Instead of finding the Schmidt pairs as continuous functions of time, we may solve this eigenvalue problem to find them in sampled data form, as the eigenvectors of the sampled Hankel matrix H. The eigenvalues of H will approach the true Hankel singular values as the

sampling time gets small. Observe that the Hankel singular value approximations are the singular values of TH, not just H. The factor of T must be retained in order to maintain the correct magnitude of the resulting singular values.

This approximation method has at least two sources of error. The most obvious error is in the sampling, or equivalently, the numerical evaluation of the integral. Although the error in the numerical approximation is readily obtainable, the relationship between this error and the resulting error in the Hankel singular values is not clear. Reducing the sampling time will increase the accuracy of the approximation, but it will also increase the size of the Hankel matrix, and will tend to make the matrix less well conditioned. The other obvious error is in the truncation of the integral. The limits of integration are from zero to infinity. Unfortunately, sampling in time out toward infinity will again yield more samples and a larger Hankel matrix. Thus this approximation method becomes a trade off. Decreasing T, or increasing N, improves the accuracy of the approximation but increases the computational complexity of the method. Again, the relationship between these time domain errors and the Hankel singular values and the Schmidt pairs is not clear.

Returning to the norms related to the Hankel operator, it is now possible to approximate the norms by using the approximate Hankel singular values found from the above numerical technique. The magnitudes of the errors in this numerical process are not known. Nevertheless, these approximations are used in the next section to obtain system error bounds.

Error Bounds based on the Approximate Hankel Operator

It is now assumed that the signal of interest is the error signal obtained by differentiating the step response as in (27). This error signal represents the impulse response of the error system. As such, it can be used to create a Hankel matrix (62), after multiplication by the sampling time T. Consequently, all the results derived so far in this section may be applied to the modeling error. These results are repeated here in terms of this error.

The Hankel norm of the modeling error is defined to be the largest Hankel singular value, which is approximated by the largest singular value of the Hankel matrix of the sampled error impulse response; that is,

$$\left\|E(s)\right\|_H \cong \hat{\sigma}_1 \ . \tag{64}$$

The nuclear Hankel norm is then approximated by the sum of the singular values of the Hankel matrix of the error impulse response; that is,

$$\|E(s)\|_{N-H} \cong \sum_{n=1}^{N} \hat{\sigma}_n \,. \tag{65}$$

The Hilbert-Schmidt Hankel norm is approximately the square root of the sum of the squares of the singular values of the sampled Hankel matrix; that is,

$$\|E(s)\|_{H-S-H} \cong \left(\sum_{n=1}^{N} \hat{\sigma}_n^2 \right)^{1/2} . \tag{66}$$

The Hilbert-Schmidt Hankel norm can also be approximated by the sampled time-weighted impulse energy using the relation

$$\|E(s)\|_{H-S-H}^2 \cong \sum_{n=1}^{N} \hat{\sigma}_n^2 \cong \sum_{k=0}^{N} kT^2 e^2(kT) \,. \tag{67}$$

The following relationships can then be applied to the various error bounds

$$\|E(s)\|_H \le \|E(j\omega)\|_\infty \le \|e\|_1 \le 2\|E(s)\|_{N-H} \,. \tag{68}$$

The Hankel norm provides a lower bound on the frequency-domain infinity-norm of the error, while the time-domain 1-norm provides an upper bound. This means that the error system Nyquist plot is certain to lie entirely within a circle of radius $\|e\|_1$, but is also certain to protrude from a circle of radius $\|E(s)\|_H$ for some frequencies. Twice the nuclear Hankel norm is an alternative upper bound on $\|E(j\omega)\|_\infty$; so, comparing $\|E(s)\|_H$, $\|e\|_1$, and $2\|E(s)\|_{N-H}$ can provide some measure of the conservativeness of the error bounds.

The Hilbert-Schmidt Hankel norm provides some independent insight into the quality of the model. Recall, for example, that $\|E(s)\|_{H-S-H}^2$ is the area enclosed by the Nyquist plot of the error system. Thus, the ratio $\|E(s)\|_{H-S-H}^2 / \|H(s)\|_{H-S-H}^2$ can be thought of as a measure of the relative Nyquist-plane modeling error.

6. MIMO Bounds

Extension of the SISO Results

The approach to the analysis of the modeling errors for multiple-input-multiple-output (MIMO) systems is similar to that described for single-input-single-output (SISO) systems in the previous sections. It is necessary first to define the MIMO error system by comparing the step-response matrix of a truth model with that of an approximate linear model. The difference between the step-response matrices is the step-response matrix of the error system. As before, this matrix of errors may be differentiated numerically to obtain the impulse-response matrix of the error system. The impulse-response matrix is written as

$$e(t) = \begin{bmatrix} e_{11}(t) & e_{12}(t) & \cdots & e_{1m}(t) \\ e_{21}(t) & e_{22}(t) & \cdots & e_{2m}(t) \\ \vdots & \vdots & \ddots & \vdots \\ e_{r1}(t) & e_{r2}(t) & \cdots & e_{rm}(t) \end{bmatrix}, \tag{69}$$

where r is the number of outputs and m is the number of inputs. The Laplace transform of $e(t)$ is the unknown error system transfer-function matrix $E(s)$.

In order to evaluate the accuracy of the MIMO model and hence its suitability for use in control system design, it is desirable to approximate the frequency-domain infinity-norm of $E(j\omega)$. This is defined as

$$\|E(j\omega)\|_\infty = \max_\omega [\sigma_{\max}\{E(j\omega)\}], \tag{70}$$

where $\sigma_{\max}\{E(j\omega)\}$ denotes the largest singular value of $E(j\omega)$. Thus the infinity-norm is the maximum value over all frequencies of the largest singular value of the error system matrix. The maximum singular value represents the largest possible ratio of the output vector magnitude to the input vector magnitude at each frequency. For the SISO case, the definition (70) reduces to the previously given definition (9), as the maximum singular value simply reduces to the magnitude of $E(j\omega)$.

A bound on $\|E(j\omega)\|_\infty$ may be obtained from the time-domain impulse-response error matrix according to the inequality

$$\|E(j\omega)\|_\infty \le \sigma_{\max}\begin{bmatrix} \|e_{11}(t)\|_1 & \|e_{12}(t)\|_1 & \cdots & \|e_{1m}(t)\|_1 \\ \|e_{21}(t)\|_1 & \|e_{22}(t)\|_1 & \cdots & \|e_{2m}(t)\|_1 \\ \vdots & \vdots & \ddots & \vdots \\ \|e_{r1}(t)\|_1 & \|e_{r2}(t)\|_1 & \cdots & \|e_{rm}(t)\|_1 \end{bmatrix}. \tag{71}$$

The 1-norm of each element of the matrix on the right can be evaluated numerically as in the SISO case. The maximum singular value of this matrix is then the bound for the frequency-domain infinity-norm. The inequality (71) is found by extension of the relation (23) as follows: Let the notation Abs[A] denote the matrix whose elements are the magnitudes of the elements of the matrix A. Then, for any frequency ω,

$$\sigma_{\max}\{E(j\omega)\} = \sigma_{\max}\left\{\int_0^\infty e(t)\exp(-j\omega t)dt\right\}$$

$$\le \sigma_{\max}\int_0^\infty \mathrm{Abs}[e(t)\exp(-j\omega t)]dt = \sigma_{\max}\int_0^\infty \mathrm{Abs}[e(t)]dt\,, \tag{72}$$

where the final integral is exactly the same as the matrix on the right-hand side of (71). Since (72) holds for any ω, it also holds when $\sigma_{\max}\{E(j\omega)\}$ is at its maximum value $\|E(j\omega)\|_\infty$; hence, (71) holds.

MIMO system norms based on the Hankel operator are defined in the same way as in the SISO case. To obtain the approximate Hankel singular values, it is necessary to construct a block Hankel matrix containing the sampled error system impulse response. The error at each sampling instant will be an $r \times m$ matrix, which will constitute one block of the Hankel matrix. The singular values of this Hankel matrix can then be used to compute approximations to any of the Hankel norms. As in the SISO case, the relations

$$\|E(s)\|_H \le \|E(j\omega)\|_\infty \le 2\|E(s)\|_{N-H} \tag{73}$$

are still valid.

Scaling of Variables

The actual value of any system norm will depend on the units chosen for the input and output variables. Therefore, it is necessary to consider the scaling of the input and output variables in order to evaluate whether a given system norm is "large" or "small." The scaling is

especially important for a MIMO system, because there is a need to compare the relative sizes of the various transfer functions that constitute the system. If the variables are poorly scaled, the effect of a single input or output may dominate the value of the system norm, and the other inputs and outputs may have almost no effect on it.

Figure 11 illustrates the scaling of the input and output variables. The actual system (or truth model) is depicted as the central block, which relates the input vector u to the output vector y. At a given operating point, the equilibrium values of u and y are denoted u_{eq} and y_{eq}, and the perturbations are denoted δu and δy, so that

$$u = u_{eq} + \delta u, \tag{74}$$

$$y = y_{eq} + \delta y. \tag{75}$$

Before the scaling, the equilibrium values u_{eq} and y_{eq} are effectively removed from consideration by use of the two summing junctions that represent (74-75). This leaves the perturbations δu and δy, which are to be related by the linear model, but which may be badly scaled. A scaling factor is included with each input and output perturbation as

$$\delta u = M_{in}\delta\bar{u}\,, \tag{76}$$

$$\delta y = M_{out}\delta\bar{y}\,. \tag{77}$$

The scaling factors are included in the diagonal matrices M_{in} and M_{out}, and are chosen so that a full-scale perturbation δu or δy corresponds to a value of ± 1 for the scaled variable $\delta\bar{u}$ or $\delta\bar{y}$. A full-scale perturbation may be taken as the largest one that would ordinarily occur, in the best estimation of the modeler. In some cases the full-scale perturbation is assumed to be the nominal equilibrium value, so that the scaled-variable values represent the percentage (or fractional) changes from the nominal values. In this case, the diagonal elements of M_{in} and M_{out} are chosen as the elements of u_{eq} and y_{eq}.

Once the appropriate scaling factors are chosen, the value of the system norm should be computed using the input and output data represented as $\delta\bar{u}$ and $\delta\bar{y}$. It is assumed that output data are collected for separate step changes applied at all the inputs. Generally, the amplitudes of the applied step changes do not correspond to unit-amplitude inputs $\delta\bar{u}$; therefore, in calculating the norm, the outputs must be scaled by the reciprocals of the amplitudes of the scaled step inputs that produced them.

7. Summary of Error Bounding Procedure

This section contains a summary of the error bounding procedure presented in the foregoing.

Step 1. Using a truth model or measured data, determine the equilibrium values of the system inputs and outputs at the desired operating point. Obtain a "truth" small-perturbation step response, and calculate δu and δy, the input and output perturbations from the equilibrium.

Step 2. Scale the small-perturbation variables δu and δy by the respective chosen scaling factors M_{in}^{-1} and M_{out}^{-1} to obtain the non-dimensional perturbations $\delta\bar{u}$ and $\delta\bar{y}$.

Step 3. Create a linear system model using some appropriate modeling method, and obtain its response $\delta\hat{\bar{y}}$ to the given scaled input perturbation $\delta\bar{u}$.

Step 4. Obtain the sampled step-error sequence $e_{step}(kT) = \delta\bar{y}(kT) - \delta\hat{\bar{y}}(kT)$.

Step 5. Numerically differentiate the step response error to obtain the error-system impulse response. This can be done by means of a simple finite difference formula such as

$$e(kT) \cong \frac{e_{step}(kT) - e_{step}((k-1)T)}{T}.$$

Step 6. To obtain the normalized (unit) impulse response of the error system, divide $e(kT)$ by the magnitude of $\delta\bar{u}$. In the MIMO case, normalize each column of the impulse-response error matrix by the magnitude of the corresponding input $\delta\bar{u}_i$. The normalization could be performed instead on $e_{step}(kT)$ in Step 4.

Step 7. Approximate the 1-norm of the normalized error-system impulse response,

$$\|e(t)\|_1 \cong \sum_{k=0}^{N} T|e(kT)|.$$

This is a bound for the frequency-domain error according to (26). It also gives a bound on the maximum output-error amplitude according to (29).

a. The model frequency response can be plotted in the Nyquist plane along with the error-bound circle plotted at the origin, as in Figure 6. The model is relatively accurate at those frequencies for which the plot is outside this circle.

b. The error bound can also be applied to the loop transfer function so as to analyze the stability robustness of a control design, as in Figures 8-10.

In the MIMO case, compute the approximate norm of each element of the error matrix, and find the bound according to (71). The Nyquist-plane interpretation is difficult in this case.

Step 8. The process can end here, or can continue using the Hankel operator. To pursue the Hankel-operator analysis, form the error-system Hankel matrix from the impulse-

response error. Find its singular values and left and right singular vectors as approximations to the Hankel singular values and Schmidt pairs, respectively.

Step 9. From the Hankel singular value approximations in Step 8, find the Hankel norm, the nuclear norm, and the Hilbert-Schmidt norm of the error system. Circles with Hankel norm radius and twice the nuclear norm radius can also be drawn in the Nyquist plane to aid in understanding the conservativeness of the bounds.

Step 10. If desired, determine the Hankel correction from the singular vector expansion in Step 8. Add the correction in parallel with the original system model to further reduce the modeling error and its bounds.

This process assumes that the deviation of the linear small perturbation model from the truth model is roughly monotonic as measured by some norm of the error. This implies that the modeling error bounds are accurate as long as the system inputs are bounded by the original step input in their time-domain infinity norms.

8. Example: A Mixed Compression Inlet

This section contains an example of the calculation of error norms in the modeling process. The system chosen is a typical mixed-compression inlet (Chicatelli and Hartley, 1997), with the downstream corrected mass flow as the input, and the static pressure just downstream of the normal shock as the output. The truth-model data is taken from the nonlinear large-perturbation CFD simulation code LAPIN (Varner et al., 1987), which uses 123 nonlinear state-variable equations for this particular case. The linearization and reduction technique presented in (Chicatelli and Hartley, 1997) provided a 16^{th}-order linear model.

A constant mass-flow input u_{eq} and a steady-state pressure output y_{eq} are taken from the LAPIN data. The scaling factor for the output perturbations is taken as

$$M_{out} = 117.8 \text{ lb/ft}^2,$$

which is the free-stream pressure. The scaling factor for the input perturbations is taken as

$$M_{in} = 1 \text{ slug/s}.$$

Truth-model data were available for a 1-% step change in the mass flow. The scaled (non-dimensional) step-response data are plotted in Figure 12 for both the truth model and the 16^{th}-order linear model. The difference between these two responses is the step response error. Dividing this error by the step-input magnitude (to normalize) and using (27) to estimate its derivative yields the error impulse response shown in Figure 13. The 1-norm of this signal is

$$\|e\|_1 = 0.4633,$$

which is a bound on the frequency-domain infinity-norm of the error system. A circle of this radius, centered at the origin, is superimposed on the frequency-response polar plot of the 16^{th}-order linear model in Figure 14. This bound is also shown on the frequency-response magnitude plot as a straight line at –6.68 dB in Figure 15. Note that the system frequency response magnitude is larger than the error bound for all frequencies up to 100 Hz. This indicates that the model will be relatively accurate within that bandwidth.

The error-system 1-norm also acts as a bound on the time-domain magnitude of any output error. According to (29), for small input variations (smaller than 1% in this case), the non-dimensional output error should remain less than 0.4633 times the non-dimensional input variation.

The approximate Hankel singular values of the error system (i.e., the singular values of the Hankel matrix of the error sequence multiplied by the sampling interval T = 0.001 s) are plotted in Figure 16. According to (64), the largest of these singular values,

$$\hat{\sigma}_1 = 0.3249,$$

represents the Hankel norm of the error system. This is a lower bound for the frequency-domain infinity-norm, meaning that the frequency-domain error magnitude is larger than this at some frequency.

The nuclear Hankel norm is approximated using (65) as

$$\sum_{n=1}^{N} \hat{\sigma}_n = 4.0688.$$

This relatively large number essentially means that any Hankel correction would have to be of high order to accomplish any significant further reduction of error. This can also be seen from the plot of the Hankel singular values in Figure 16, which reveals that cutting the Hankel-norm error in half would require at least a sixth-order correction.

The Hilbert-Schmidt Hankel norm (or Frobenius Hankel norm) is approximated using (66) as

$$\left(\sum_{n=1}^{N} \hat{\sigma}_n^2 \right)^{1/2} = 0.8444.$$

Recall that the area enclosed by the Nyquist plot of the error system is equal to the square of this Hilbert-Schmidt Hankel norm, or 0.7130. By comparison, the area enclosed by the Nyquist plot of the system model $H(s)$ itself is found to be 0.9018.

9. Conclusion

The step response of a system may be readily available, even when the impulse response and the frequency-domain description are not. This paper has shown how some time-domain and frequency-domain bounds useful in modeling and control design may be determined from the system step response. The calculation of the bounds requires first a numerical differentiation of the step-response error to estimate the impulse-response error. A frequency-domain error bound may then be determined by use of a simple numerical integration. The Hankel norms of the error system may also be determined from a Hankel matrix of the impulse-response error, by use of singular-value calculations. The Hankel-norm information may be used to compute some additional frequency-domain upper and lower bounds, to determine an error-reducing correction to a given model, and to qualitatively evaluate the relative frequency-domain modeling error in the Nyquist plane.

References

S. P. Boyd and C. H. Barratt, *Linear Controller Design: Limits of Performance*, Prentice-Hall, 1991.

A. Chicatelli and T. T. Hartley, "A Method for Generating Reduced Order Linear Models of Supersonic Inlets," NASA Contractor Report 198538, January 1997.

J. C. Doyle, B. A. Francis, and A. R. Tannenbaum, *Feedback Control Theory*, MacMillan, 1992.

K. Glover, R. F. Curtain, and J. R. Partington, "Realization and Approximation of Linear Infinite-Dimensional Systems with Error Bounds," *SIAM J. Control & Optimization*, vol. 26, no. 4, pp. 863-898, July 1988.

K. Glover and J. R. Partington, "Bounds on the Achievable Accuracy in Model Reduction," in NATO ASI Series, vol. F34, *Modeling, Robustness, and Sensitivity Reduction in Control Systems*, R.F. Curtain, ed., Springer-Verlag, 1987.

B. Hanzon, "The Area Enclosed by the (Oriented) Nyquist Diagram and the Hilbert-Schmidt-Hankel Norm of a Linear System," *IEEE Trans. Automatic Control*, vol. 37, no. 6, pp. 835-839, June 1992.

M. O. Varner, et al, "Large Perturbation Flow Field Analysis and Simulation for Supersonic Inlets: Program Modifications," Sverdrup Technology, Contract NAS3-24105, April 1987.

W. V. Lovitt, *Linear Integral Equations*, Dover, 1950.

J. R. Partington, *An Introduction to Hankel Operators*, Cambridge University Press, 1988.

Appendix: Matlab code listing for computing example error bounds

```
% FILE norms.m
%
% Data file 'normdata' contains scaled output data from the truth
% model (ynl), and unscaled output data from the 16th-order model (yr).
load normdata
T=time(10)-time(9);
%
% Plot truth-model and 16th-order model step responses
figure(12)
plot(time,ynl(:,1),'o',time,ynl(1,1)+yr(:,1))
xlabel('Time (seconds)')
ylabel('Scaled (non-dimensional) pressure')
text(0.953,10.03,'o  truth model')
text(0.953,10.01,'-  16th-order linear model')
grid
%
% Calculate scaled (non-dimensional) error.
e=(ynl(:,1)-ynl(5,1)*ones(size(yr(:,1))))-yr(:,1);
%
% Differentiate to find impulse-response error.
ei=diff(e)/T;
% Divide by step-input magnitude to normalize ei
ei=ei/((input(190)-input(5)));
%
% Plot scaled, normalized inpulse-response error.
figure(13)
plot(time(1:196),ei,'b')
ylabel('Scaled, normalized impulse-response error')
xlabel('Time (seconds)')
grid
%
% Compute one-norm of the impulse-response error.
onenorm=sum(abs(ei))*T
%
% Calculate coordinates of circle in complex plane.
j=sqrt(-1);
w=[-180:180]*pi/180;
cir=onenorm*exp(j*w);
%
% Calculate frequency response of 16th-order model.
sysr=ss(ar,br,cr(1,:),dr(1,:));
wr=logspace(0,4,200);
[rfr,ifr]=nyquist(sysr,wr);
% Scale the frequency response: 117.8 is the freestream pressure
% This scaling was not built into the 16th-order model
rfr=rfr/117.8;
ifr=ifr/117.8;
%
% Make polar plot with circle to show error bound.
figure(14)
plot(rfr,ifr)
axis equal
hold on
plot(real(cir),imag(cir),'r')
```

```
ylabel('Imaginary H(jw)')
xlabel('Real H(jw)')
grid
hold off
%
% Make magnitude plot with line to show error bound.
figure(15)
wr=logspace(0,3,200);
[rfr,ifr]=nyquist(sysr,wr);
rfr=rfr/117.8;
ifr=ifr/117.8;
semilogx(wr/6.28,20*log10(sqrt(rfr.*rfr+ifr.*ifr)))
hold on
semilogx(wr/6.28,20*log10(onenorm*ones(size(rfr))),'r')
xlabel('Frequency (Hz)')
ylabel('Frequency-response magnitude (dB)')
grid
hold off
%
% Construct Hankel matrix from impulse-response error sequence.
h=hankel(ei);
% Truncate matrix to eliminate zeros.
m=length(ei)/2;
h=h(1:m,1:m);
% Calculate Hankel singular values
[u,s,v]=svd(h);
% Put Hankel singular values into a vector
s=diag(s*T);
%
% Plot Hankel singular values.
figure(16)
plot(s,'o')
grid
ylabel('Hankel singular value')
xlabel('Singular value number')
%
% Calculate Hankel norms.
hnorm=s(1)
nnorm=sum(s)
hsnorm=sqrt(sum(s.*s))
```

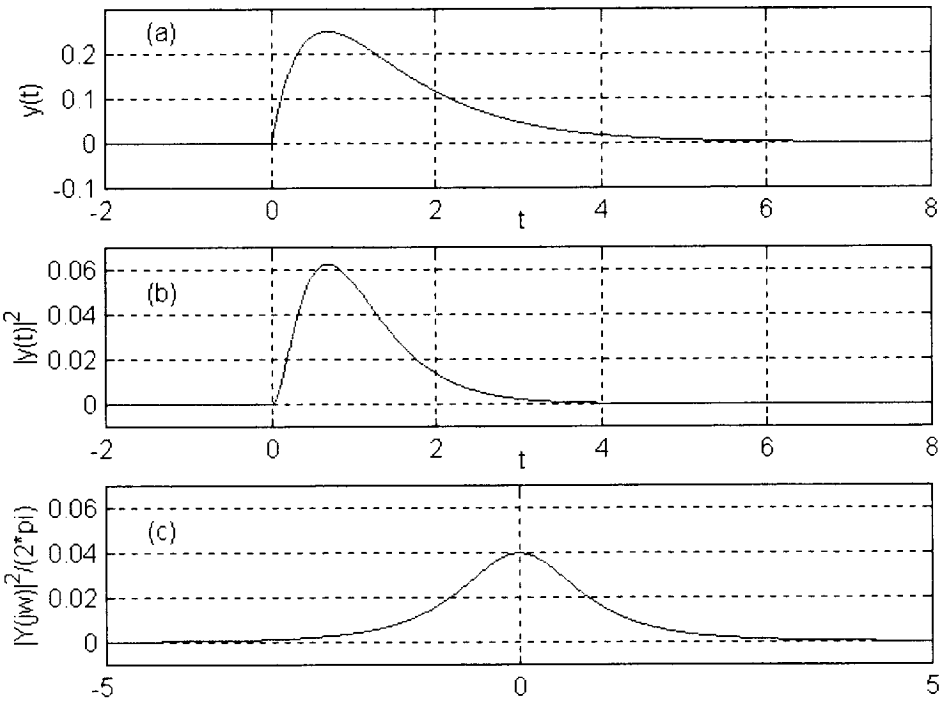

Figure 1. Functions to illustrate time-domain and frequency-domain norms.

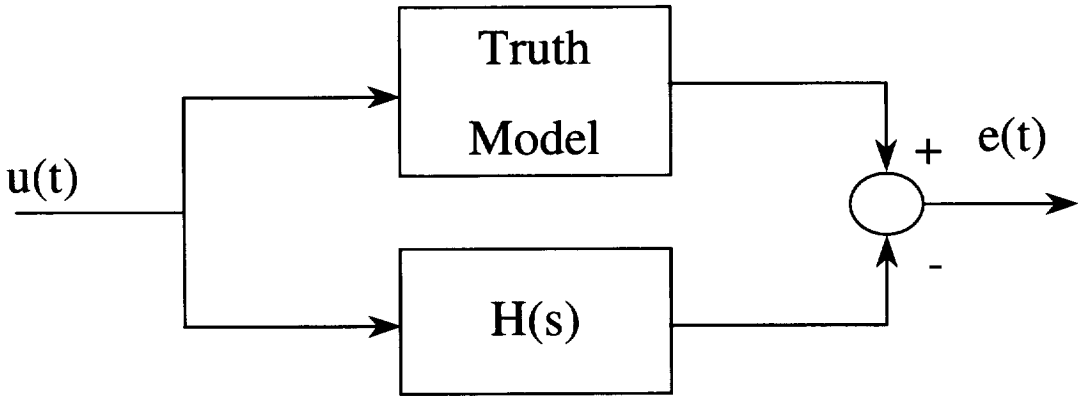

Figure 2. The error system.

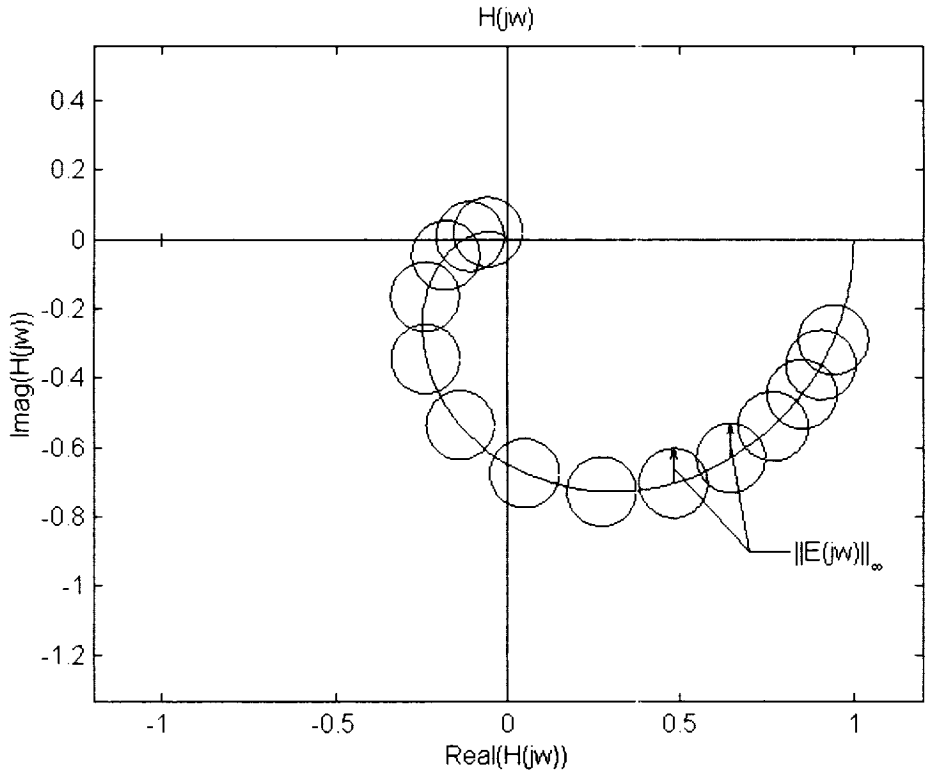

Figure 3. Frequency-domain error bound represented in the Nyquist plane.

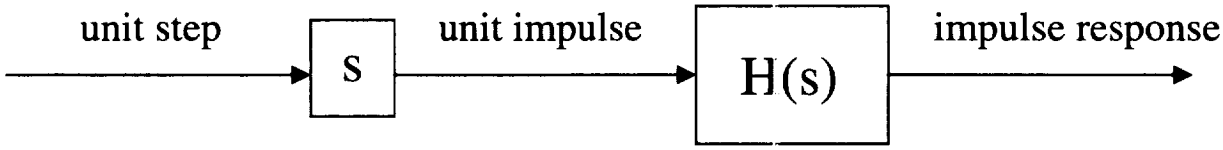

Figure 4. Obtaining the system impulse response the hard way.

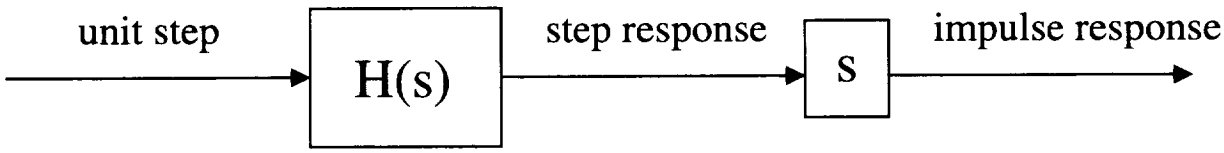

Figure 5. Obtaining the system impulse response the easy way.

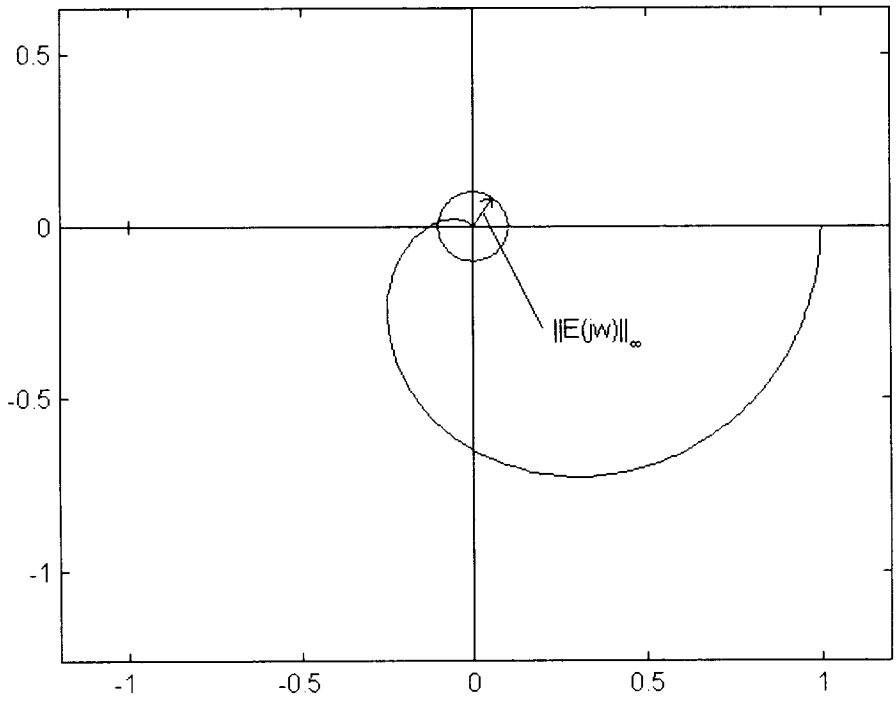

Figure 6. Frequency-domain error bound represented in the Nyquist plane, revisited.

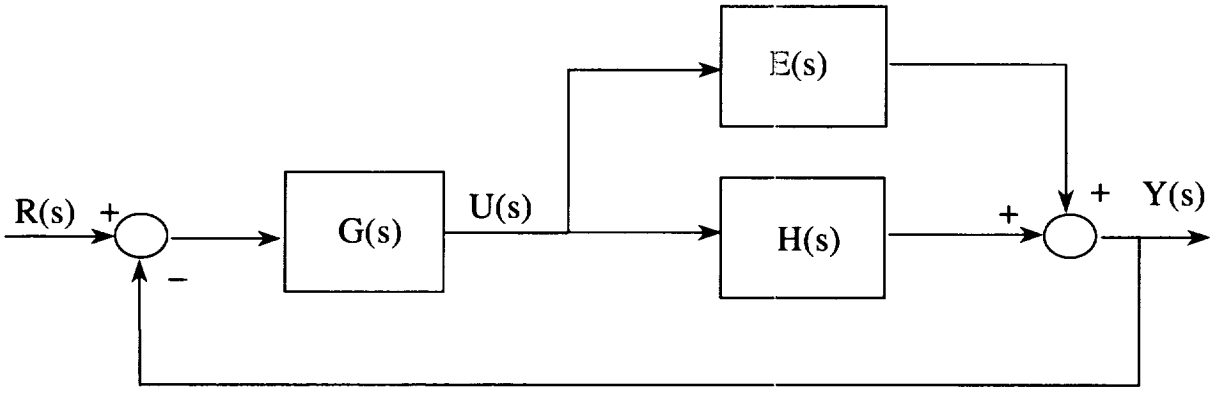

Figure 7. Closed-loop system with unmodeled dynamics included.

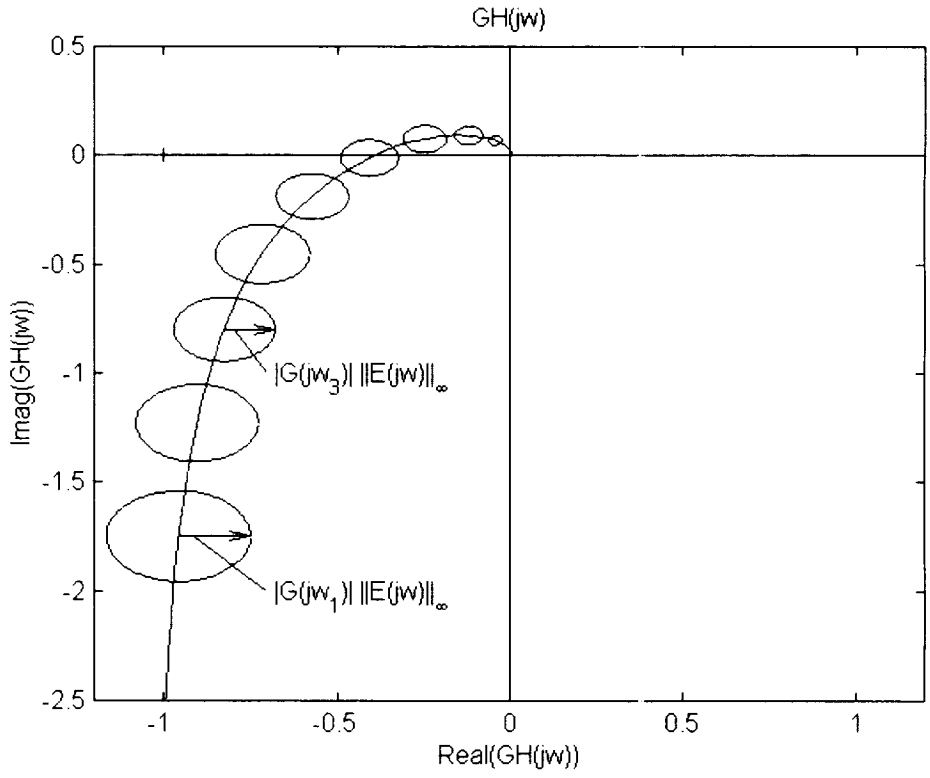

Figure 8. Frequency-dependent error bounds represented in the Nyquist plane.

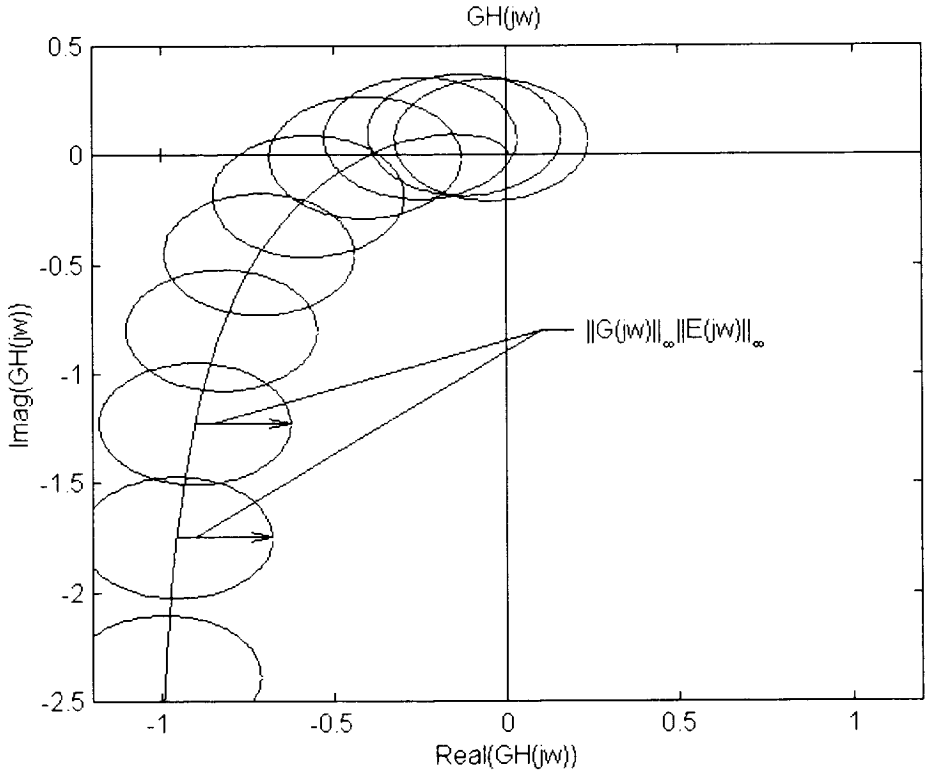

Figure 9. Worst-case error bound represented in the Nyquist plane.

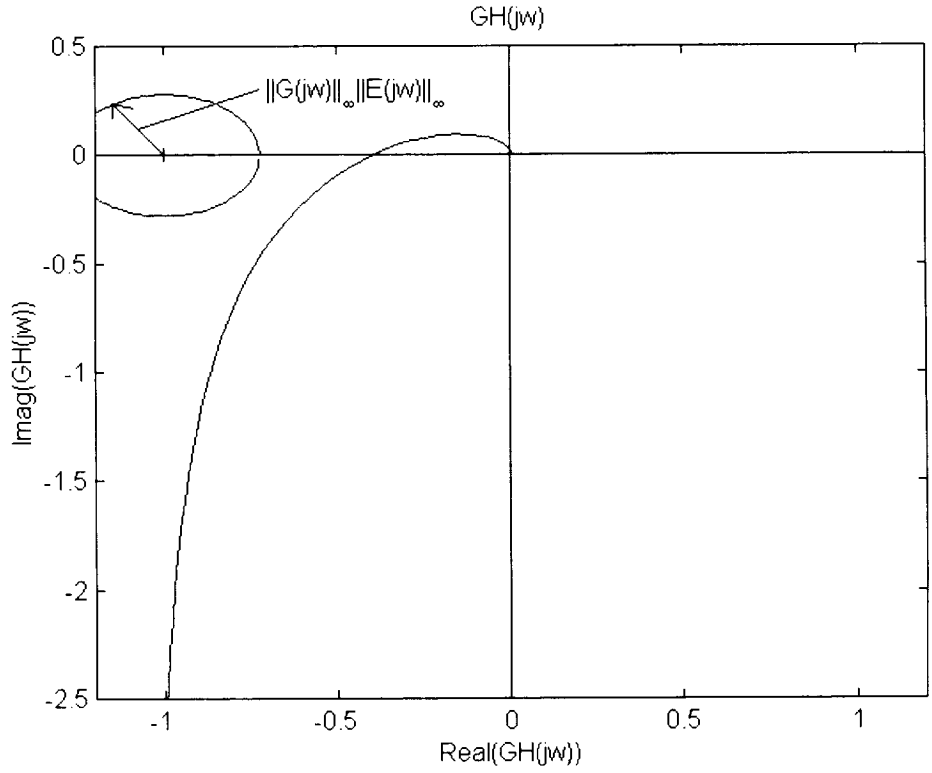

Figure 10. Worst-case error bound represented in the Nyquist plane, revisited.

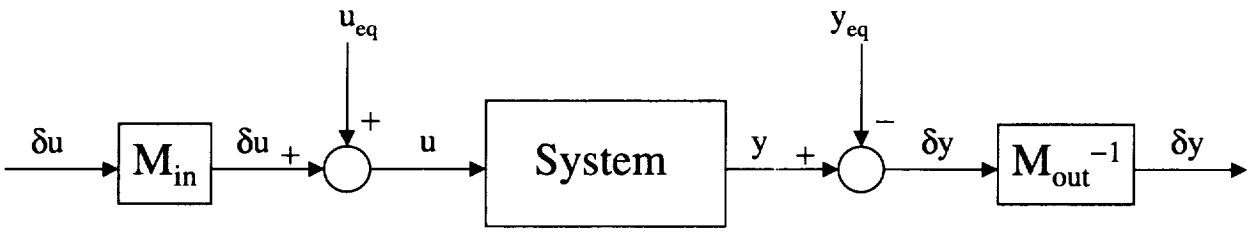

Figure 11. Scaling of the input and output variables.

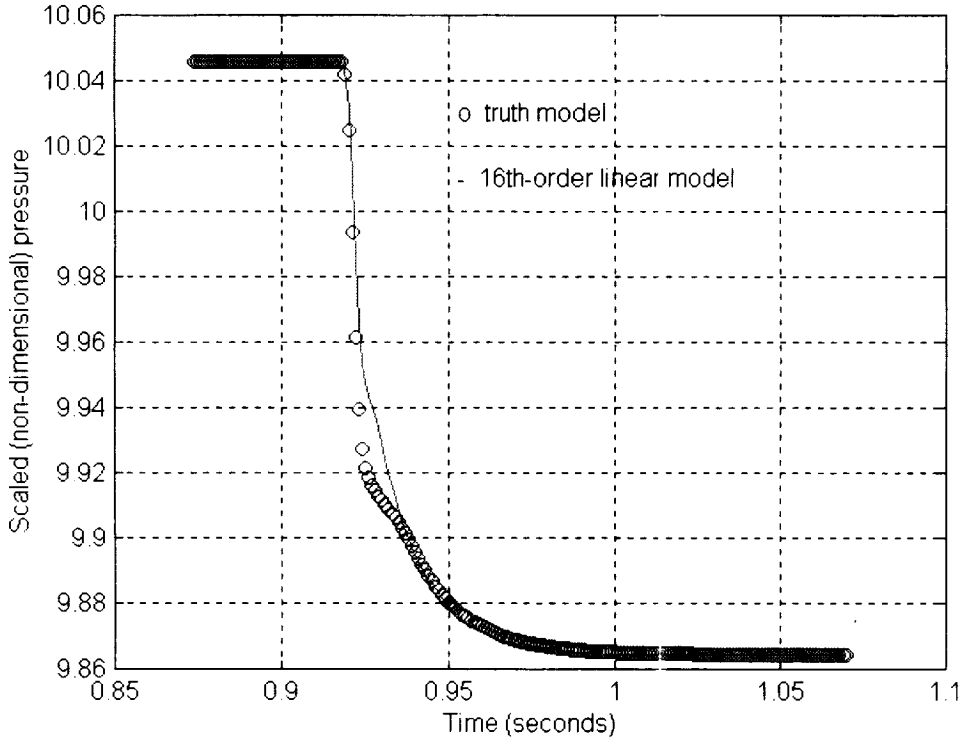

Figure 12. Step responses of truth model and 16th-order linear model.

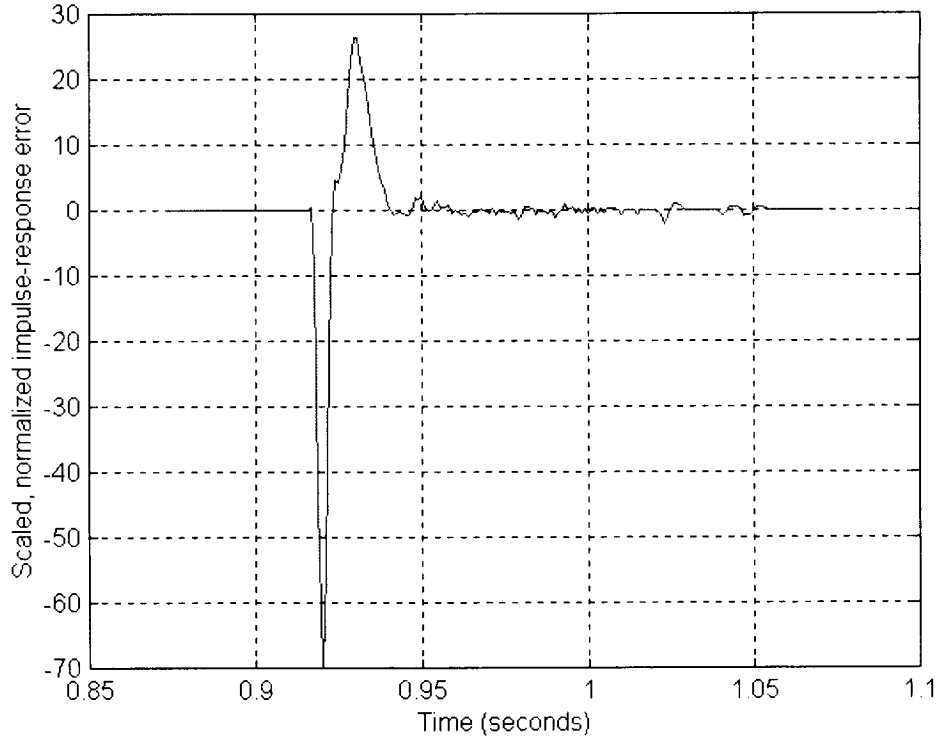

Figure 13. Impulse response error found by numerical differentiation of the step response error.

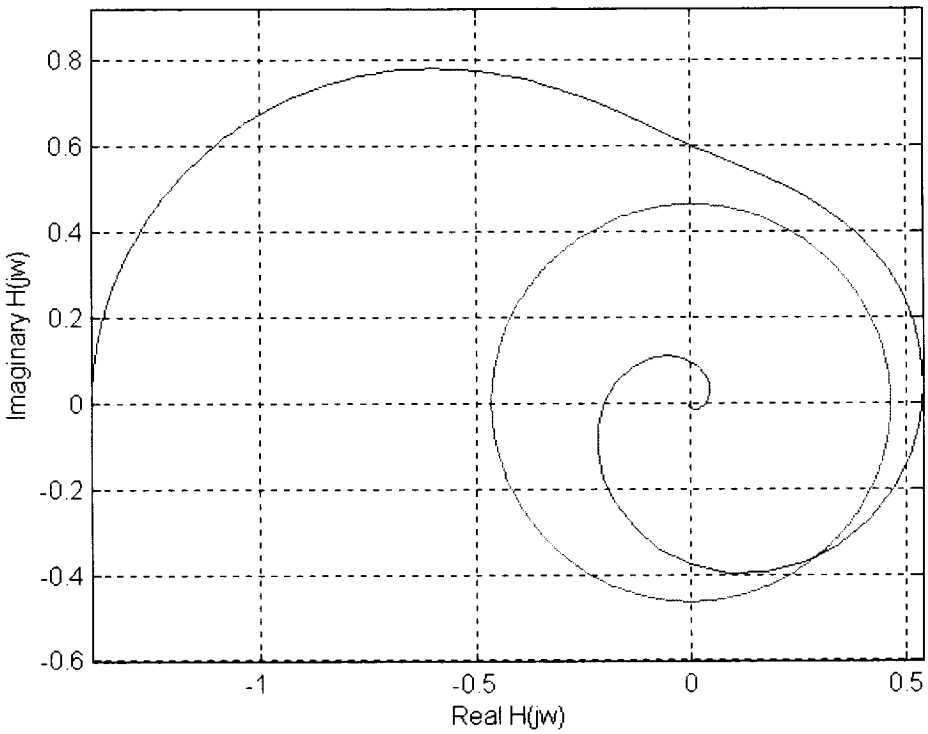

Figure 14. Polar plot of frequency response of 16^{th}-order model.

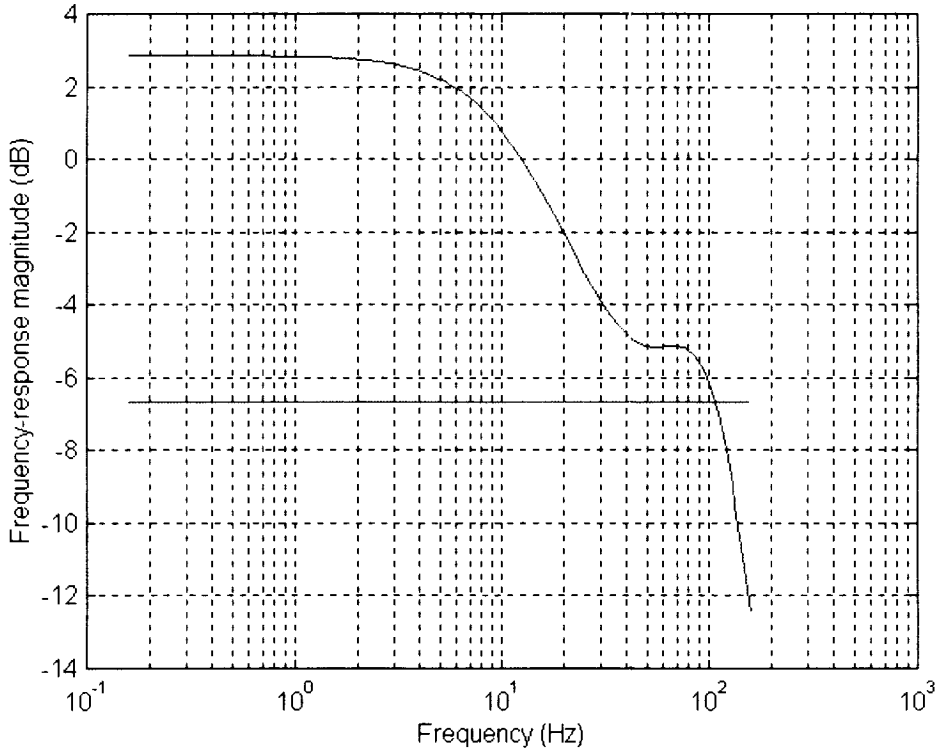

Figure 15. Magnitude plot of frequency response of 16th-order model.

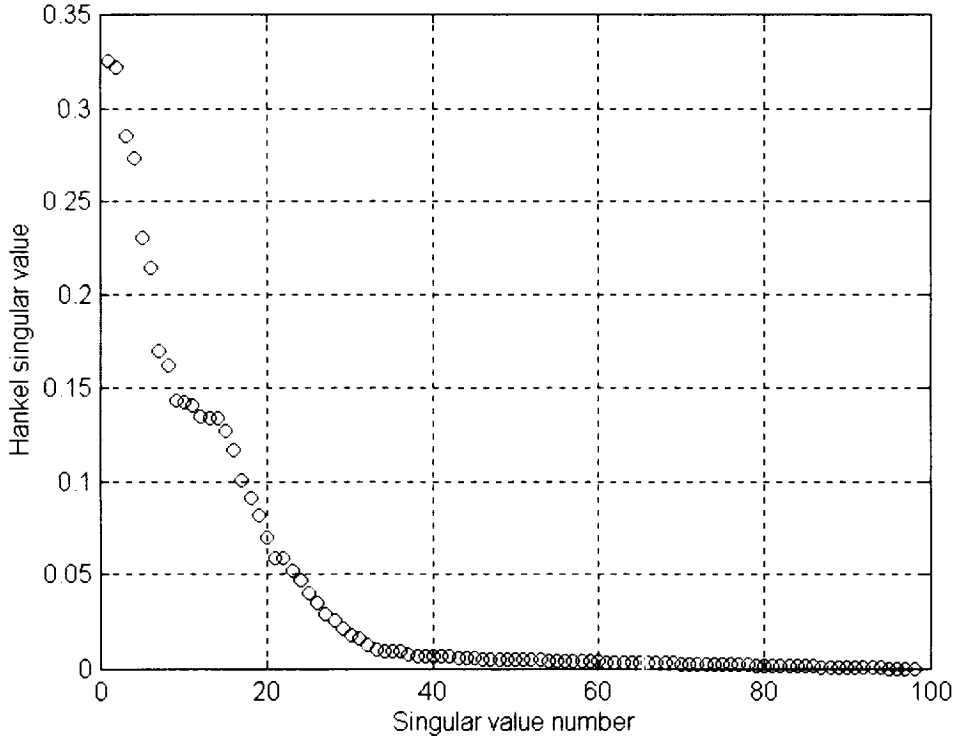

Figure 16. Hankel singular values of the error system.

REPORT DOCUMENTATION PAGE

Form Approved
OMB No. 0704-0188

1. AGENCY USE ONLY (*Leave blank*)	2. REPORT DATE	3. REPORT TYPE AND DATES COVERED
	August 1998	Final Contractor Report

4. TITLE AND SUBTITLE

To Err is Normable: The Computation of Frequency-Domain Error Bounds From Time-Domain Data

5. FUNDING NUMBERS

WU–519–30–53–00
NCC3–508

6. AUTHOR(S)

Tom T. Hartley, Robert J. Veillette, J. Alexis De Abreu Garcia, Amy Chicatelli, and Richard Hartmann

7. PERFORMING ORGANIZATION NAME(S) AND ADDRESS(ES)

University of Akron
Department of Electrical Engineering
Akron, Ohio 44325–3904

8. PERFORMING ORGANIZATION REPORT NUMBER

E–11295

9. SPONSORING/MONITORING AGENCY NAME(S) AND ADDRESS(ES)

National Aeronautics and Space Administration
Lewis Research Center
Cleveland, Ohio 44135–3191

10. SPONSORING/MONITORING AGENCY REPORT NUMBER

NASA CR—1998-208516

11. SUPPLEMENTARY NOTES

Project Manager, Kevin J. Melcher, Instrumentation and Controls Division, NASA Lewis Research Center, organization code 5530, (216) 433–3743.

12a. DISTRIBUTION/AVAILABILITY STATEMENT

Unclassified - Unlimited
Subject Categories: 08 and 63 Distribution: Nonstandard

This publication is available from the NASA Center for AeroSpace Information, (301) 621–0390.

12b. DISTRIBUTION CODE

13. ABSTRACT (*Maximum 200 words*)

This paper exploits the relationships among the time-domain and frequency-domain system norms to derive information useful for modeling and control design, given only the system step response data. A discussion of system and signal norms is included. The proposed procedures involve only simple numerical operations, such as the discrete approximation of derivatives and integrals, and the calculation of matrix singular values. The resulting frequency-domain and Hankel-operator norm approximations may be used to evaluate the accuracy of a given model, and to determine model corrections to decrease the modeling errors.

14. SUBJECT TERMS

Error analysis; H-infinity control; MIMD (control systems); Dynamic models; Mathematical models

15. NUMBER OF PAGES

44

16. PRICE CODE

A03

17. SECURITY CLASSIFICATION OF REPORT	18. SECURITY CLASSIFICATION OF THIS PAGE	19. SECURITY CLASSIFICATION OF ABSTRACT	20. LIMITATION OF ABSTRACT
Unclassified	Unclassified	Unclassified	